NeuroImage 116 (2015) 102–111

Contents lists available at ScienceDirect

NeuroImage

journal homepage: www.elsevier.com/locate/ynimg

# Conflict awareness dissociates theta-band neural dynamics of the medial frontal and lateral frontal cortex during trial-by-trial cognitive control

Jun Jiang [a,b], Qinglin Zhang [a,*], Simon van Gaal [b,c,**]

[a] Key Laboratory of Cognition and Personality (Ministry of Education), and Faculty of Psychology, Southwest University, Chongqing, China
[b] University of Amsterdam, Department of Psychology, The Netherlands
[c] Donders Institute for Brain, Cognition and Behavior, The Netherlands

ARTICLE INFO

*Article history:*
Received 11 November 2014
Accepted 29 April 2015
Available online 6 May 2015

ABSTRACT

Recent findings have refuted the common assumption that executive control functions of the prefrontal cortex exclusively operate consciously, suggesting that many, if not all, cognitive processes could potentially operate unconsciously. However, although many cognitive functions can be launched unconsciously, several theoretical models of consciousness assume that there are crucial qualitative differences between conscious and unconscious processes. We hypothesized that the potential benefit of awareness in cognitive control mechanisms might become apparent when high control has to be maintained across time and requires the interaction between a set of distant frontal brain regions. To test this, we extracted oscillatory power dynamics from electroencephalographic data recorded while participants performed a task in which conflict awareness was manipulated by masking the conflict-inducing stimulus. We observed that instantaneous conflict as well as across trial conflict adaptation mechanisms were associated with medial frontal theta-band power modulations, irrespective of conflict awareness. However, and crucially, across-trial conflict adaptation processes reflected in increased theta-band power over dorsolateral frontal cortex were observed after fully conscious conflict only. This suggests that initial conflict detection and subsequent control adaptation by the medial frontal cortex are automatic and unconscious, whereas the routing of information from the medial frontal cortex to the lateral prefrontal cortex is a unique feature of conscious cognitive control.



## Introduction

Many perceptual and cognitive functions can be influenced by subliminal information and in recent years it has been shown that even "high-level" executive functions (i.e. error/conflict processing, task-set switching, response inhibition) can be launched unconsciously (for reviews, see Desender and Van Den Bussche, 2012; van Gaal and Lamme, 2012). These findings contradict the commonly held assumption that executive functions of the prefrontal cortex exclusively operate consciously (for reviews, see Badgaiyan, 2000; Dehaene and Naccache, 2001; Eimer and Schlaghecken, 2003; Hommel, 2007; Jack and Shallice, 2001; Norman and Shallice, 1986). More speculatively, these results might even suggest that all cognitive processes can potentially operate in two separate modes: a conscious one and an unconscious one.

However, although unconscious processes seem very powerful, there might be crucial differences between conscious and unconscious executive processes. We hypothesize that these become evident when increased levels of control have to be maintained for longer periods of time and conflict adaptation requires the information exchange between distant prefrontal brain regions. Previous studies have shown that subliminal information processing is fleeting (decaying within ~500 ms Greenwald et al., 1996) and restricted to local processing modules (van Gaal and Lamme, 2012). According to the global neuronal workspace theory (Dehaene and Naccache, 2001), conscious information processing, on the other hand, is associated with strong and durable neuronal firing and relies on the sharing and routing of information among several high-level inter-connected cortical regions, among which the dorsolateral prefrontal cortex (DLPFC) seems to play a crucial role (Dehaene et al., 2014).

To test the potential benefit of awareness and the role of the DLPFC in trial-by-trial executive control processes (as compared to online transient control), we extracted oscillatory neural dynamics from current-source density transformed EEG data recorded while human participants performed a typical "conflict task" in which conflict awareness was manipulated by masking (Fig. 1A). Conflict tasks (i.e. Stroop, Flanker) are often performed to study conflict monitoring/detection mechanisms on the current trial as well as trial-by-trial conflict-

* Correspondence to: Q. Zhang, Faculty of Psychology, Southwest University, Beibei, Chongqing, 400715, China.
** Correspondence to: S. van Gaal, University of Amsterdam, Department of Psychology, Weesperplein 4, 1018 XA, Amsterdam, The Netherlands.
*E-mail addresses:* qlzhang.swu@gmail.com (Q. Zhang), simonvangaal@gmail.com (S. van Gaal).

http://dx.doi.org/10.1016/j.neuroimage.2015.04.062
1053-8119/

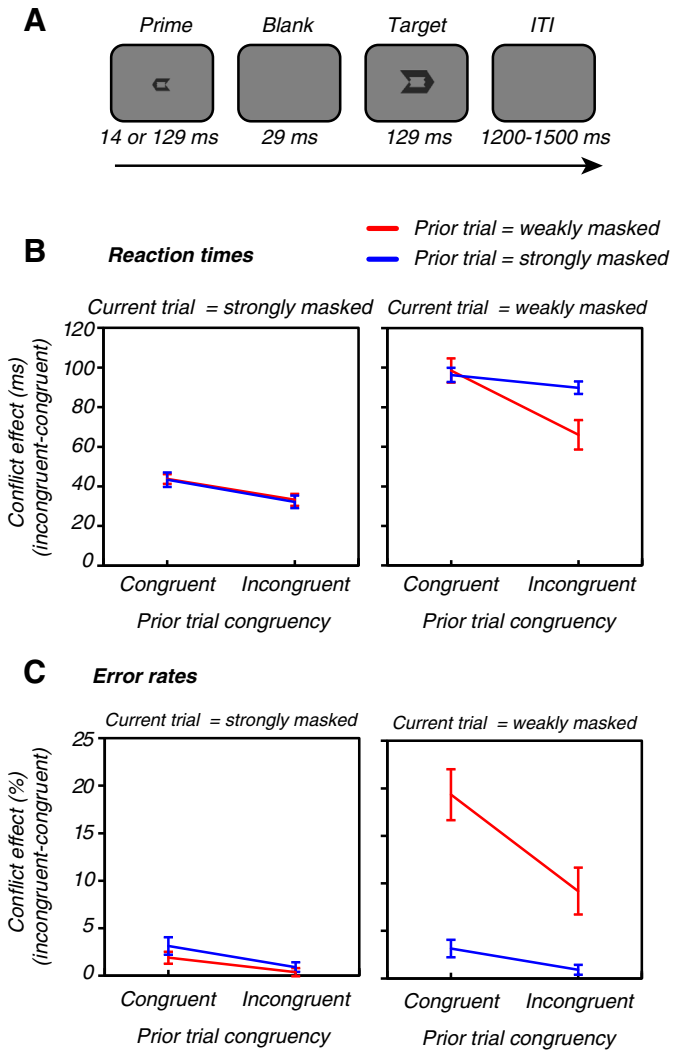


**Fig. 1.** Experimental design and behavioral results. (A) Schematic representation of the experimental task and the stimuli. Primes could be congruent or incongruent with the direction of the target (50/50 congruent/incongruent trials). Primes could be presented briefly (14 ms, strongly masked primes) or longer (129 ms, weakly masked primes). (B/C) Conflict adaptation effects for different levels of masking strength in the prior and current trial. Conflict effects in trial $n$ for RTs (mean RT on incongruent trials–mean RT on congruent trials, B) and error rates (mean percentage of errors on incongruent trials–mean percentage of errors on congruent trials, C) as a function of prime-target correspondence in trial $n-1$ (congruent vs. incongruent), masking strength in trial $n$ (weak vs. strong masking) and masking strength in trial $n-1$. Error bars reflect the standard error of the mean.

induced control adaptations on the next trial (the "Gratton" effect, Gratton et al., 1992). The underlying neural sources of conflict resolution are studied extensively and there are several models trying to explain the phenomenon (Egner, 2007). The conflict-monitoring model proposes that the medial frontal cortex (MFC) and the anterior cingulate cortex (ACC) in particular, monitor or detect the presence of conflict and then signal other regions, most prominently the DLPFC, to subsequently implement cognitive control (Botvinick et al., 2001; MacDonald et al., 2000). Others have argued for a control-implementing or "regulatory" role, in contrast to a mere "monitoring" role, of the ACC instead (Posner and DiGirolamo, 1998; Roelofs et al., 2006). Theta-band neural dynamics over midfrontal/dorsolateral frontal cortex are thought to be a candidate mechanism for the realization of cognitive control (Cavanagh and Frank, 2014). It seems that it is especially the DLPFC that has a mnemonic function in maintaining information about recently experienced conflict in order to modify the control level the next time conflict occurs (Mansouri et al., 2009). The maintaining of conflict information over time might be a mechanism that requires high levels of consciousness, because unconscious information processing seems fleeting and quickly decaying across time (decaying <500 ms) (Dehaene et al., 2003; Dehaene and Naccache, 2001; Greenwald et al., 1996; van Gaal et al., 2010a). Therefore, based on previous studies and theoretical models, we hypothesized that ACC-mediated conflict detection/resolution processes might be operational independent of conflict awareness, whereas DLPFC-mediated trial-by-trial conflict adaptation processes could be uniquely operational when conflict is experienced fully consciously.

## Methods

### *Participants*

Twenty-one undergraduate students (11 females) aged between 18 and 25 ($M = 21.7$, SD = 1.95), recruited from the Southwest University (Chongqing, China) participated in this experiment for monetary compensation. All participants were right-handed, had normal or corrected-to-normal vision, and had no history of head injury or physical and mental illness. This study was approved by the local ethics committee of Southwest University, and written informed consent was obtained from all participants after the explanation of the experimental protocol.

### *Design and procedures*

Dark gray (RGB: 40, 40, 40) stimuli were presented against a lighter gray (RGB: 128, 128, 128) background at the center of a 17-inch Lenovo VGA monitor (frequency 70 Hz, resolution 1024 × 768) with the E-prime 1.1 software package (Psychology Software Tools, Pittsburgh, PA). Participants were seated 70 cm from the computer screen. An arrow version of the meta-contrast masked priming task was used (Kunde, 2003; van Gaal et al., 2010a). The left and right arrows (visual angle of 0.82° × 0.57°) served as primes, and the somewhat larger left and right arrows (visual angle of 1.96° × 1.31°) served as targets (Fig. 1A). The primes fitted exactly within the inner contour of the target and therefore the targets served as meta-contrast masks, strongly affecting stimulus visibility.

The prime was either presented for 14 ms or for 129 ms and was always followed by a blank screen lasting 29 ms. Subsequently the target was presented for 129 ms. The inter-trial interval had a variable duration (1200–1500 ms) in which the subject had to respond. Half of the primes were strongly masked, and half of the time weakly masked. Participants were instructed to ignore the prime and to respond to the direction of the target arrow as quickly and accurately as possible by pressing the "F" with the left index finger (for a left target), or the "J" with the right index finger (for a right target) on a QWERTY keyboard. Fifty percent of all trials were congruent and 50% were incongruent.

Before the actual experiment, participants performed one practice block with 24 trials containing performance feedback (mean RT and percentage correct were displayed on the computer screen after each trial). Thereafter, subjects performed 8 experimental blocks of 192 trials each (1536 trials in total).

The visibility of the primes was determined by a force-choice discrimination task (192 trials, 50/50 strongly/weakly masked) at the end of the experiment. The timing was the same as in the actual experiment with the exception that after each trial a screen was inserted after the target to ask the participants to discriminate the direction of the prime arrow. To exclude the possibility that the participants responded based on the target direction rather than the direction of prime arrow in the strongly masked condition, the target arrow was replaced by a neutral arrow, which was made by overlapping the left-pointing and right-pointing target arrows. All trials were presented randomly, and strongly/weakly masked primes were mixed in current study. To more precisely evaluate the visibility of the primes, we also recruited an independent cohort of 25 subjects (14 females) who each conducted two blocks of a post discrimination task: one block was completely

identical to the task mentioned above, in the other block the targets were left or right arrow targets (as in the EEG experiment) rather neutral targets.

### *Behavioral data analysis*

The first trial of each block, incorrect and missed trials, trials following an error and correct trials with an RT <100 or >1000 ms were excluded from all analyses (10.39% in total, the mean percentage and SD of rejected trials per condition are reported in Supplementary Table S1). To be clear, we thus only included "correct trial pairs". We were especially interested in whether the conscious experience of response conflict on trial $n-1$ (prior trial) influenced cognitive control mechanisms on trial $n$ (current trial). We expected that the correspondence effect on trial $n$ (incongruent-congruent of the current trial) would be smaller when trials are preceded by an incongruent trial compared to a congruent trial; here referred to as *conflict adaptation* (Egner, 2007; Gratton et al., 1992; van Gaal et al., 2010a).

Reaction times (RTs) and error rates (ERs) were entered into separate repeated measures ANOVAs with 4 factors: visibility in the prior trial (strongly/weakly masked primes), prior trial congruency (congruent vs. incongruent), visibility in the current trial, and current trial congruency (all within-subject variables). A one sample *t*-test on *d′*, an objective bias-free measure of a subjects' ability to detect a signal (Wickens, 2002), was used to analyze prime visibility. A two-tailed significance level of 0.05 was used for all tests.

### *EEG measurements and preprocessing*

Participants were seated in a dimly lit and electrically shielded room and were asked to avoid eye blinks and movements during the task. EEG activity was recorded from 64 scalp sites using tin electrodes mounted in an elastic cap (Brain Products, Munich, Germany). The vertical electro-oculogram (EOG) was recorded from an electrode below the right eye. The horizontal EOG was collected from an electrode located at the outer canthus of the right eye. EEG and EOG signals were filtered using a 0.01–100 Hz band-pass and continuously sampled at 500 Hz. All electrode impedance was kept below 5 kΩ by careful preparation.

The preprocessing was conducted using custom-made MATLAB (R2009a, The MathWorks, Inc.) scripts supported by EEGLAB (Delorme and Makeig, 2004). Continuous EEG data were first offline digitally filtered with band-pass between 0.5 and 30 Hz and referenced to the average of the activity recorded at the left and right mastoids, and then segmented from −1.5 s to 2 s around target onset in each trial. The epochs corresponding to the behavioral exclusion criteria and epochs deviating more than 5 SD from the mean probability distribution were excluded (Jiang et al., 2013). Thereafter, independent components (ICs) were calculated to isolate artifacts contained in the EEG signal. With the EEGLAB plugin ADJUST (Mognon et al., 2011), ICs representing eye blinks, eye movements, muscle artifacts, or other types of noise were removed from the EEG signal (Delorme and Makeig, 2004).

### *Time frequency decomposition*

Before time frequency transformation, all clean EEG data were current-source-density (CSD) transformed. CSD is a spatial filter that minimizes volume-conducted effects and increases topographical selectivity by effectively removing spatially broad signals. The method has been validated in previous EEG studies (e.g., Cavanagh et al., 2009; Cohen and van Gaal, 2013; Cohen et al., 2009; Mansfield et al., 2012). Single-trial EEG data of each condition were decomposed into their time–frequency representations (TFRs) from 1 Hz to 30 Hz in 30 logarithmically spaced steps using custom-made Matlab scripts, which first multiply the power spectrum of the EEG (obtained from the fast Fourier transform) by the power spectrum of complex Morlet wavelets ($e^{-i2\pi tf}e^{-t^2/(2\sigma^2)}$), where t is time, f is frequency, and σ defines the width of each frequency band, which was set as 3–10 logarithmically spaced cycles to trade-off temporal and frequency resolution, and then taking the inverse fast Fourier transform. From the complex signal, we estimated the frequency band-specific power at each time point, defined as the squared magnitude of the result of the convolution Z ($\mathrm{real}[z(t)]^2 + \mathrm{imag}[z(t)]^2$) (see Cohen and van Gaal, 2013). The TFRs of each subject of each condition were averaged to identify the modulations by conflict on the current trial (I–C) and further to identify the conflict adaptation effect on the next trial (conflict effect after congruent trials–conflict effect after incongruent trials, or (cI–cC)–(iI–iC)). The averaged power was transformed using a decibel (dB) scale and normalized using the common baseline (averaged across all conditions, −300 ms to −100 ms preceding the target) activity for each estimated frequency according to the equation: dB power = 10 * log10 (power/baseline) (Cohen and van Gaal, 2013). Conversion to a dB scale ensures that data across all frequencies, time points, electrodes, conditions, and subjects are in the same scale and thus visually and statistically comparable.

### *Time frequency power analysis: Confirmatory analyses*

Based on previous studies, including our own, we expected to observe midfrontal theta dynamics related to conflict (Cavanagh et al., 2009; Cavanagh and Frank, 2014; Cohen et al., 2008; Nigbur et al., 2012) and conflict adaptation (Pastötter et al., 2013; Tang et al., 2013). To extract these dynamics we used a fronto-central region of interest (ROI) where these effects tend to peak, including electrodes (Fz, FCz, Cz). For the conflict adaptation DLPFC hypothesis we could not formulate a specific hypothesis regarding the lateralization of the effect, because previous studies have observed both right-lateralized (Egner and Hirsch, 2005; Greene et al., 2004; Kerns, 2006; Kerns et al., 2004) as well as left-lateralized (Cavanagh et al., 2009; Cohen and van Gaal, 2013; Kerns, 2006; Kim et al., 2013, 2014; Nigbur et al., 2012; Salami et al., 2014) DLPFC conflict adaption effects. Therefore, we looked at two spatial ROIs, either on the left (AF7, F5, F7) or right (AF8, F6, F8) side, both containing three electrodes over lateral prefrontal cortex (Cavanagh et al., 2009; Nigbur et al., 2012).

First, we defined the time–frequency region of interest for the specific analysis of interest. For current trial conflict this was I–C, averaged across all visibility conditions and prior trial congruency. For conflict adaptation this was (cI–cC)–(iI–iC) averaged across all visibility conditions. On these contrasts, statistics were performed by *t*-tests, and multiple comparisons were corrected using cluster-based permutation testing (TF region: −200 to 1200 ms and 1–30 Hz) (Cohen and van Gaal, 2014; Maris and Oostenveld, 2007), in which the assignment of condition to each data point was randomly shuffled, and statistics were re-computed. After thresholding each permutation map ($p = 0.001$), the number of pixels in the largest supra-threshold cluster was stored. This was repeated 2000 times, generating a distribution of maximum cluster sizes under the null hypothesis. Any clusters in the real data that were at least as large as the 95% of the distribution of null hypothesis cluster sizes were considered statistically significant. Then, subsequent ANOVAs were performed using the observed significant time–frequency ROIs (or masks) to test for potential interactions with masking strength. For the current trial effect we perform ANOVAs with the factors Current Trial Congruency and Current Trial Masking. For the across trial effects we perform ANOVAs with the factors Current Trial Congruency, Prior Trial Congruency, Current Trial Masking and Prior Trial Masking. Note that the interaction between Current Trial Congruency and Prior Trial Congruency is referred to as *conflict adaptation*.

### *Time frequency power analysis: Exploratory analyses*

The contrast incongruent vs. congruent trials on the current trial (the conflict effect) revealed not only theta-band dynamics, but also

alpha/beta modulations at centro-parietal (ROI of FCz, Cz, Cpz, P1, P2) (see also Pastötter et al., 2013 for a similar observation) and parieto-occipital electrodes (ROI of P7, P5, P3, P1, Pz, P2, P4, P6, P8, PO7, PO3, POz, PO4, PO8, O1, Oz, O2) (see Compton et al., 2011, 2012 for a similar observation). These effects survived multiple comparisons corrections using cluster-based correction methods at a $p < 0.001$. To test for interactions of conflict and conflict adaptation with visibility, a similar procedure was used as described for theta.

*Source reconstruction analysis*

We further examined the potential sources of the reported theta modulations related to overall conflict (Fig. 2A) and conflict adaptation, specifically the difference of conflict adaptation when the prior trial was strongly masked vs. weakly masked (Fig. 3C). Source reconstructions for each subject were separately performed using the Brainstorm package (Tadel et al., 2011), which is documented and freely available for download online under the GNU general public license (http://neuroimage.usc.edu/brainstorm). Time–frequency ROIs for the source reconstructions were defined by the significant T-F clusters observed in Figs. 2A and 3C. Sources were estimated using depth weighted minimum-norm estimation (MNE) using a three-shell sphere forward model (unconstrained). As individual brain images were not obtained, MNE was performed on the default anatomical MNI template implemented in Brainstorm ("Colin27") using the default sensor locations for each individual. *t*-tests were performed to estimate the statistical significance across individuals.

## Results

*Prime discrimination*

The results of the post-discrimination task directly performed after the EEG measurements (neutral target arrows) showed that the visibility of the masked primes was higher for weakly masked ($d' = 1.59$, SD = 0.74, $d'$ range: 0.43–2.92, corresponding to 77% correct on average) than strongly masked primes ($d' = 0.03$, SD = 0.14, $d'$ range: −0.26–0.21, corresponding to 50.6% correct on average, $t_{20} = 9.83$, $p < 0.001$). Discrimination performance on strongly masked primes ($d'$) was not significantly higher than zero ($t_{20} = 1.08$, $p = 0.294$), which was the case for weakly masked primes ($t_{20} = 9.81$, $p < 0.001$). Further, as revealed by a binominal test, none of the subjects scored above chance-level (all $ps > 0.17$). These results suggest that participants were unable to recognize the direction of the prime arrows consciously in the strongly masked condition. However, based on the relatively low performance in the weakly masked condition (77% correct), we were concerned that subjects were not performing optimal in the post-discrimination task, possibly due to fatigue, because the discrimination task was performed after the actual EEG experiment (after about 2 h of testing). Therefore, we performed an additional visibility test in a new cohort of 25 participants (see Methods). In this new group, the visibility of the weakly masked primes was indeed higher ($d' = 2.91$, SD = 0.87, $d'$ range: 1.15–4.07, corresponding to 91.8% correct on average), which was also the case for the strongly masked primes ($d' = 0.30$, SD = 0.67, $d'$ range: −1.07–1.73, corresponding to 55.7% correct on average, difference: $t_{24} = 14.79$, $p < 0.001$). Although $d'$ was low on strongly masked trials, it was above chance-level ($t_{24} = 2.28$, $p = 0.032$), which was also the case for weakly masked primes ($t_{24} = 16.72$, $p < 0.001$). In the block in which the target was a left- or right-pointing arrow (see Methods), performance was similar. Performance was higher for the weakly masked condition ($d' = 2.87$, SD = 0.84, $d'$ range: 0.98–4.07, 90.8% correct on average) than the strongly masked condition ($d' = 0.18$, SD = 0.32, $d'$ range: −0.36–1.04, 53.3% correct on average, difference: $t_{24} = 16.11$, $p < 0.001$) and in both conditions $d'$ was significantly higher than zero (strongly masked: $t_{24} = 2.75$, SD = 0.84, $p = 0.011$; weakly masked: $t_{24} = 17.19$, $p < 0.001$).

Overall, the discrimination results show that our masking procedure was successful in creating two clearly different prime visibility conditions. The results also suggest that the primes in the strongly masked condition cannot be considered to be fully unconscious on the group level, as we have observed in previous studies using similar masking procedures (Jiang et al., 2013; van Gaal et al., 2011). Therefore, we will refer to these conditions as weakly masked vs. strongly masked conflict from now on. We have performed a series of Spearman rank correlations between $d'$ scores (from the main experiment) and behavioral and EEG measures for the strongly masked condition to explore the relation between the reported effects and prime visibility, which are reported at the end of the Results section.

*Behavioral performance*

Repeated measures ANOVA on response times (RTs) and error rates (ERs) revealed a main effect of current trial congruency (RT: $F_{1,20} = 327.98$, $p < 0.001$; ER: $F_{1,20} = 46.63$, $p < 0.001$), indicating that participants responded faster and made fewer errors when the trial was congruent (RT: $M = 373$ ms, SE = 10.01; ER: $M = 0.77\%$, SE = 0.83%) than when it was incongruent (RT: $M = 436$ ms, SE = 11.49; ER: $M = 9.31\%$, SE = 6.07%). This conflict effect (I–C, current trial) was modulated by prime visibility on the current trial (RT: $F_{1,20} = 59.28$, $p < 0.001$; ER: $F_{1,20} = 37.23$, $p < 0.001$). Further, the conflict effect was smaller when the prior trial was incongruent compared to when it was congruent: an index of conflict adaptation (RT: $F_{1,20} = 66.78$, $p < 0.001$, ER: $F_{1,20} = 20.35$, $p < 0.001$). This result reveals the conflict adaptation effect across all levels of visibility in the prior and the current trial. However, the conflict adaptation effect was larger when the prime of the prior trial was weakly masked than when it was strongly masked (RT: $F_{1,20} = 20.13$, $p < 0.001$; ER: $F_{1,20} = 11.07$, $p = 0.003$). Furthermore, the conflict adaptation effect was modulated not only by the visibility of the prior trial, but also by the visibility of the current trial, as shown by the four-way interaction (RT: $F_{1,20} = 21.82$, $p = 0.019$; ER: $F_{1,20} = 14.31$, $p < 0.001$). Four separate two-way repeated measures ANOVAs (for all possible combinations of visibility in the prior and the current trial) further revealed that conflict adaptation was present for all levels of prime visibility in the prior and the current trial (RT: all $Fs > 5.24$; all $ps < 0.033$; ER: all $Fs > 4.85$; all $ps < 0.04$). Although present for all possible combinations of stimulus visibility in the prior and current trial, the conflict adaptation effect was strongest when the visibility of both the prior trial and the current trial were high (Figs. 1B and C, see also Supplementary Tables S2 and S3 for mean RTs and mean ERs for all 16 conditions, respectively), replicating previous behavioral findings (van Gaal et al., 2010a).

*Theta power dynamics of conflict (current trial effects)*

As expected, stimulus-locked time–frequency dynamics for conflict on the current trial (I–C, averaged across all visibility conditions and prior trial congruency) revealed a strong power increase at midfrontal electrodes, peaking in the theta-band, replicating previous studies (Fig. 2, peak frequency = 6.5 Hz, frequency range = 2.9–13.2 Hz, time range = −10–780 ms) (Cavanagh et al., 2009; Cavanagh and Frank, 2014; Nigbur et al., 2012; Pastötter et al., 2013; Tang et al., 2013). We extracted oscillatory power from this time–frequency region of interest (specified in Fig. 2A) for further ANOVAs on the midfrontal ROI with the factors Current Trial Masking and Current Trial Congruency. Besides the main effect of Congruency reported above ($F_{1,20} = 82.92$, $p < 0.001$), this analysis revealed a main effect of Current Trial Masking (stronger theta response for weakly masked compared to strongly masked condition: $F_{1,20} = 61.53$, $p < 0.001$) and an interaction between Current Trial Masking and Current Trial Congruency, indicating that the conflict effect was stronger for weakly masked conflict than for strongly masked conflict ($F_{1,20} = 29.89$, $p < 0.001$, see Fig. 2B iv and C). Follow-up separate ANOVAs per Current Trial Masking condition with the factor Current

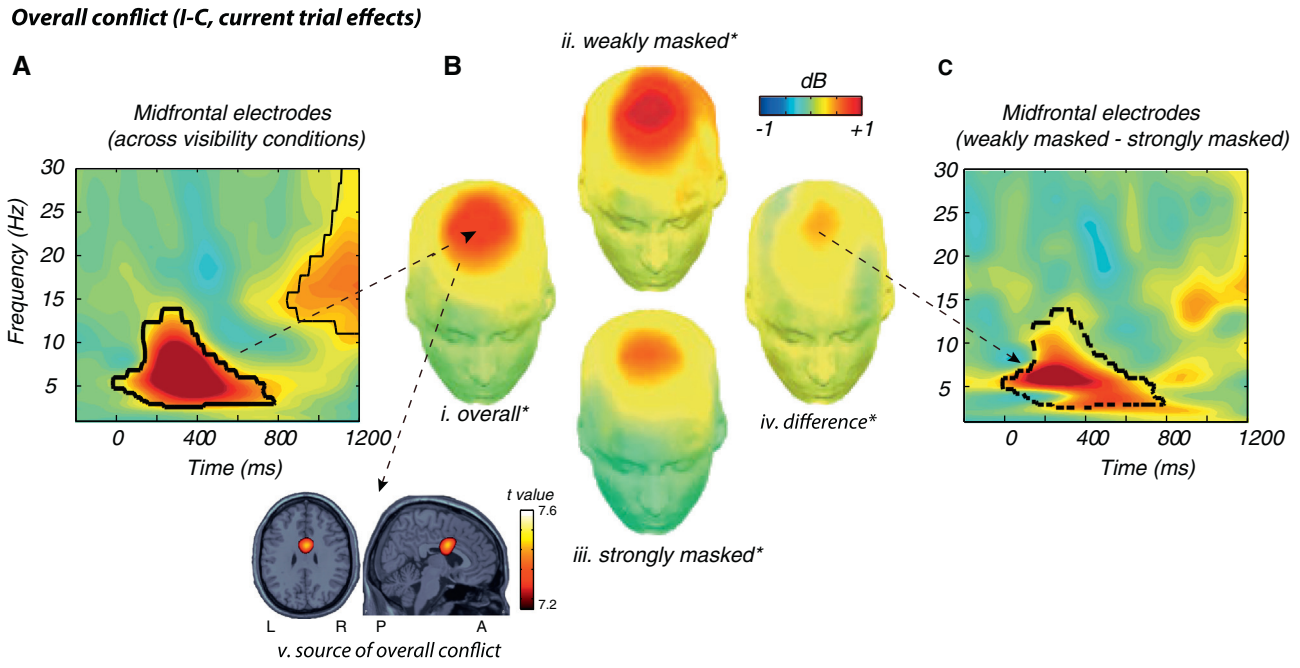


**Fig. 2.** Current trial conflict effects at midfrontal electrodes. (A) Time–frequency power dynamics of overall conflict at midfrontal electrodes (Cz, FCz, Fz) (I–C, averaged across prime visibility on the prior/current trial and prior trial congruency). Time 0 is the onset of the target arrow. Black lines encircle regions of significance at $p < 0.001$, corrected for multiple comparisons using cluster based statistics. Theta-band power data in the enclosed area (with arrow) were used for all topographical plots (scaling: −1.5 to +1.5 dB). (B) Topographical distributions for the theta-band conflict effect at the current trial are reported across all masking conditions (i.), separated by conflict masking strength on the current trial (ii. and iii.) and for the difference between weakly masked and strongly masked conflict (iv.). *Reflects $p < 0.05$ for the relevant comparison. (C) The time–frequency plot of the difference between weakly and strongly masked conflict for midfrontal electrodes (scaling: −1.5 to +1.5 dB). The observed theta difference between strongly masked conflict and weakly masked conflict trials was significant ($F_{1,20} = 29.9$, $p < 0.001$). The TF region of interest used for testing is highlighted by the dotted line. This TF region was defined by the significant main effect of conflict across all visibilities observed in (A).

Trial Congruency revealed that conflict-evoked theta was present both on weakly masked ($F_{1,20} = 70.71$, $p < 0.001$) and strongly masked conflict conditions ($F_{1,20} = 72.59$, $p < 0.001$, see Fig. 2B ii and iii). Source reconstruction of the overall conflict theta-band effect (shown in A) suggests that the source of this effect was likely in the medial frontal cortex (peak MNI coordinate: $x = 4$, $y = 3$, $z = 29$), replicating previous studies (see reviews Cavanagh and Frank, 2014; Nigbur et al., 2011; Pastötter et al., 2013).

*Alpha/Beta power dynamics of conflict (current trial effects)*

We also observed conflict-related modulations in two other time–frequency bands, namely a suppression of occipito-parietal power in a broad alpha/beta-band (peaking in high alpha ~400–600 ms) and an increase in centro-parietal alpha/beta-band activity in the inter-trial interval (peaking in beta ~800–1200 ms), leading up to the next trial (Compton et al., 2011, 2012; van Driel et al., 2012). Because our a priori hypotheses mainly regarded frontal theta modulations, we first explored the across-trial theta-band dynamics in more detail. Thereafter, we will further discuss the alpha/beta-band effects, which were more exploratory in nature. To be sure, these alpha/beta-band effects were strong and survived multiple comparisons corrections (FDR) across time, frequency and electrodes and are shown here for the electrodes where these effects peaked, consistent with previous study (Pastötter et al., 2013).

*Theta power dynamics of conflict adaptation at midfrontal electrodes (across trial effects)*

Next, we zoomed in on the frontal theta-band dynamics related to conflict adaptation, plotted as the TF difference of the conflict effect (current trial) after congruent and incongruent trials ((cI–cC)–(iI–iC)) (Fig. 3A). Conflict adaptation (averaged across visibility conditions in the prior/current trial) was clearly observed in the theta range at midfrontal electrodes (Fig. 3A, headmap i. in Fig. 3B, frequency range = 5.2–10.4 Hz, time range = 230–540 ms, $p < 0.001$, corrected for multiple comparisons). Next, we extracted oscillatory power from this time–frequency region of interest for further ANOVAs with the factors Current Trial Masking, Current Trial Congruency, Prior Trial Masking, and Prior Trial Congruency. We only focus on the effects related to conflict adaptation (note that the current trial effects are reported above). Besides the conflict adaptation effect reported above (interaction between Prior Trial Congruency and Current Trial Congruency: $F_{1,20} = 45.44$, $p < 0.001$), conflict adaptation was modulated by Prior Trial Masking: it was stronger after weakly masked than strongly masked trials ($F_{1,20} = 5.68$, $p = 0.027$). We also observed a main effect of Prior Trial Congruency ($F_{1,20} = 15.61$, $p = 0.001$) and a 3-way interaction between Prior Trial Masking, Prior Trial Congruency and Current Trial Congruency ($F_{1,20} = 8.21$, $p = 0.001$). No other effects were significant (all $ps > 0.05$).

Planned follow-up analyses separating conflict adaptation based on whether the prior conflict was weakly masked or strongly masked, revealed significant conflict adaptation effects for both conditions (Fig. 3B, weakly masked: $F_{1,20} = 38.44$, $p < 0.001$, headmap ii.; strongly masked: $F_{1,20} = 19.31$, $p < 0.001$, headmap iii.).

*Theta power dynamics of conflict adaptation at lateral frontal electrodes (across trial effects)*

Interestingly, an ANOVA on the left lateral frontal ROI with all 4 factors also revealed theta-band conflict adaptation effects ($F_{1,20} = 7.13$, $p = 0.015$) and also that conflict adaptation was modulated by Prior Trial Masking ($F_{1,20} = 10.82$, $p = 0.004$). This latter effect indicates that conflict adaptation was stronger when prior conflict was weakly masked than when it was strongly masked (Fig. 3B, headmap iv., see also the TF map in Fig. 3C for the frequency specificity of this effect, ROI of electrodes AF7, F7, and F5). There was also an interaction

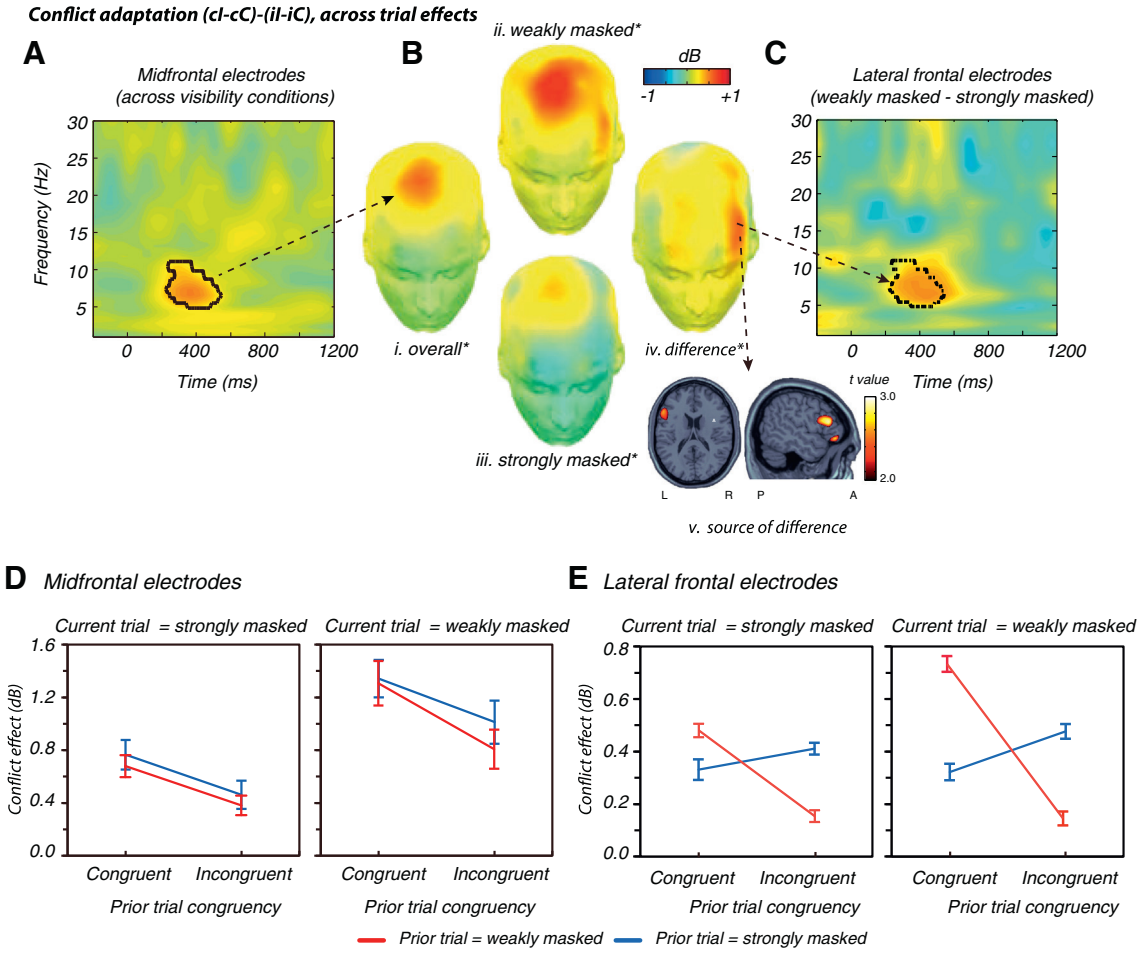


**Fig. 3.** Conflict adaptation effects at midfrontal and left lateral frontal electrodes. (A) Time–frequency power dynamics of overall conflict adaptation ((cI–cC)–(iI–iC)) averaged across all masking conditions on the prior/current trial. Time 0 is the onset of the target arrow. Black lines encircle regions of significance at $p < 0.001$, corrected for multiple comparisons using cluster based statistics. The time–frequency data in the enclosed area were used for all topographical plots (scaling of TF map: −1.5 to +1.5 dB). The significant time–frequency region of interest (all pixels encircled in A) was used to test for theta-modulations at lateral frontal electrodes (see dotted line ROI in C). (B) Topographical distributions for the theta conflict adaptation effect are reported across all masking conditions (i.), separated by masking strength on the prior trial (ii. and iii.) and for the difference between weakly masked and strongly masked conflict on the prior trial (iv.). *Reflects $p < 0.05$ for the relevant comparison. (C) The time–frequency power plots for the difference between conflict adaptation for weakly masked and strongly masked conflict in the prior trial were significant at left lateral frontal electrode sites (AF7, F7, F5; $F_{1,20} = 10.8$, $p = 0.004$), but not at right lateral frontal electrodes (AF8, F8, F6). The dotted line encircles the TF region that was used for testing. Note that this TF region was obtained from an independent analysis (A). (D) Line plots for the conflict effect at midfrontal electrodes, separated by masking strength on the prior and current trial, and congruency on the prior trial. A negative slope of the lines reflects a conflict adaptation effect. (E) Line plots for the conflict adaptation effect separated by masking strength on the prior and current trial at left lateral frontal electrodes. A negative slope of the lines reflects a conflict adaptation effect. Error bars reflect the standard error of the mean.

between Prior Trial Masking and Prior Trial Congruency ($F_{1,20} = 6.10$, $p = 0.023$). No other effects were significant (all $ps > 0.05$).

Two follow-up ANOVAs for each Prior Trial Masking condition revealed that when the prior conflict was weakly masked, theta-band power modulations were significant at left lateral prefrontal electrode sites ($F_{1,20} = 15.43$, $p < 0.001$, Fig. 3B headmap ii.). Interestingly, this lateral prefrontal effect was absent when the prior trial was a strongly masked conflict trial ($F_{1,20} = 1.43$, $p = 0.247$, headmap iii.). If anything, the DLPFC effect for conflict adaptation after strongly masked conflict was in the opposite direction, suggesting that this null-effect was not due to a lack of statistical power. Source reconstruction confirmed that the main difference between conflict adaptation initiated after weakly masked and strongly masked conflict originated from the left lateral prefrontal cortex (peak MNI coordinate: $x = -51$, $y = 22$, $z = 13$, see Fig. 3C).

The conflict adaptation-related theta-band modulation was specific for *left* lateral frontal electrodes and did not reach significance at *right* lateral frontal electrode sites (2-way interaction Current Trial Congruency and Prior Trial Congruency: $F_{1,20} = 2.99$, $p = 0.099$), regardless of whether prior conflict was weakly masked ($F_{1,20} = 2.02$, $p = 0.171$) or strongly masked ($F_{1,20} = 1.01$, $p = 0.327$). Thus, conflict adaptation-related theta-band modulations were clearly present at midfrontal electrodes when awareness of prior conflict was high and low, whereas left dorsolateral frontal theta-band effects were uniquely observed after fully conscious conflict in the prior trial.

### *Alpha/Beta-band modulations*

We also observed a power decrease in the alpha/beta-band at occipito-parietal electrodes after conflict compared to no conflict (averaged across all visibility conditions), peaking in alpha (peak frequency = 11.7 Hz, frequency range = 8.3–21.1 Hz, time range = 230–680 ms, Fig. 4A, $F_{1,20} = 85.3$, $p < 0.001$, corrected for multiple comparisons) (see Compton et al., 2011, 2012 for a similar observation). An ANOVA with all 4 factors revealed that this effect was also modulated by Current Trial Masking ($F_{1,20} = 81.68$, $p < 0.001$). No other effects were significant (all $ps > 0.05$).

Separate ANOVAs revealed that that this Current Trial Conflict effect was significant both for strongly masked ($F_{1,20} = 41.70$, $p < 0.001$) and weakly masked primes ($F_{1,20} = 100.71$, $p < 0.001$) in the current

trial. No differences were observed related to conflict adaptation ($F_{1,20} = 1.09$, $p = 0.308$ across all visibility conditions). These results indicate that the alpha-band conflict-related power decrease was present both for weakly and strongly masked conflict, but that this effect was not modulated by prior trial congruency (and/or the visibility of the prior or current trial, see also Fig. 4C).

Additionally, there was a relative alpha/beta-band power conflict-related increase at centro-parietal electrodes, peaking in the beta-band (peak frequency = 16.7 Hz, frequency range = 9.3–30 Hz, time range = 802–1200 ms) leading up to the next trial (Fig. 4B/D, $F_{1,20} = 52.84$, $p < 0.001$, averaged across visibility conditions, corrected for multiple comparisons) (see also Pastötter et al., 2013 for a similar observation). This current trial conflict effect was stronger for weakly masked conflict than strongly masked conflict ($F_{1,20} = 21.79$, $p < 0.001$), but separate ANOVAs revealed it was present for weakly masked conflict ($F_{1,20} = 50.54$, $p < 0.001$) as well as strongly masked conflict ($F_{1,20} = 28.75$, $p < 0.001$).

There was also a two-way interaction between Prior Trial Congruency and Current Trial Congruency averaged across all visibility conditions, reflecting conflict adaptation ($F_{1,20} = 4.48$, $p = 0.047$). However, Prior Trial Masking and Current Trial Masking did not affect this conflict adaptation effect (no other effects were significant, all $ps > 0.05$).

*Correlational analyses between behavior and EEG*

To further qualify the relationship between behavioral and oscillatory data we performed several rank correlational analyses (Spearman). First, we correlated the current trial conflict-related midfrontal theta-band power effect with the conflict effect in reaction times and error rates (incongruent–congruent). We observed significant positive across-subject correlations between these measures for both weakly masked (RTs: $r_s = 0.53$, $p = 0.012$; ERs: $r_s = 0.53$, $p = 0.013$) and strongly masked conflict (RTs: $r_s = 0.46$, $p = 0.036$; not significant for ERs: $r_s = 0.16$, $p = 0.491$, see Supplementary Fig. S1 for scatter plots). Further, we did not observe significant (positive) correlations between the behavioral conflict adaptation effects and the left DLPFC theta-power effects, neither for weakly masked, nor for strongly masked trials (all $r_s < 0.13$, see Supplementary Fig. S2).

Next, we explored whether the reported behavioral and EEG effects were driven by visibility of the primes, which did not seem to be the case. The $d'$ scores were not systematically correlated with the behavioral measures of interest (conflict effect: RTs: $r_s = 0.29$, $p = 0.197$; ERs: $r_s = 0.17$, $p = 0.462$; conflict adaptation effect: RTs: $r_s = 0.26$, $p = 0.257$; ERs: $r_s = -0.04$, $p = 0.862$) and the EEG measures of current trial conflict (MFC conflict: $r_s = -0.07$, $p = 0.76$) or across trial conflict adaptation (MFC conflict adaptation: $r_s = 0.01$, $p = 0.97$; left DLPFC conflict adaptation: $r_s = -0.04$, $p = 0.853$).

## Discussion

Here we demonstrate that oscillatory theta-band power dynamics in the human medial frontal and dorsolateral prefrontal cortex dissociate across-trial conflict processing at different levels of conflict awareness. In line with previous observations, instantaneous conflict on the current trial elicited a typical early medial frontal theta-band power increase, accompanied by conflict-related behavioral slowing. This effect was present both for weakly masked and strongly masked conflict (Fig. 2). Furthermore, conflict-induced behavioral adjustments on the next trial (Gratton effect in behavior) were present both after strongly masked as well as weakly masked conflict in the prior trial. However, these behavioral modulations were much stronger after weakly masked conflict that after strongly masked conflict, in line with previous findings (Ansorge et al., 2011; Desender et al., 2013; Kunde, 2003; van Gaal et al., 2010a). Medial frontal theta-band power modulations related to conflict adaptation were also observed after strongly and weakly masked conflict in the prior trial. However, importantly, dorsolateral frontal conflict-induced theta-band modulations on the next trial were uniquely observed after weakly masked (fully conscious) conflict, and were absent after strongly masked conflict in the prior trial.

Recently it has been proposed that the trial-by-trial adaptation of behavior according to the history of recently experienced conflict requires a mnemonic system that allows for the maintenance of information about experienced conflict across trials (Horga et al., 2011; Mansouri et al., 2009). This memory component of conflict processing is supposed to be encoded in the activity of DLPFC neurons (Mansouri et al., 2007). Another line of theorizing proposes the existence of two qualitative different modes of cognitive control that arise because of different temporal dynamics: reactive and proactive control (Braver, 2012). In these models, reactive control reflects stimulus-driven transient forms of cognitive control, whereas proactive control is associated with trial-by-trial and anticipatory control mechanisms, which are strongly associated with the lateral prefrontal cortex. Interestingly, influential models of consciousness also assert a crucial role for the lateral prefrontal cortex in durable and global conscious information sharing and routing, which is supposed to rely on a set of interconnected high-level cortical areas forming a 'global neuronal workspace' (Dehaene et al., 2014).

Here we attempt to reconcile these models of conflict monitoring/resolution with models of consciousness. In light of the abundance of studies showing a crucial role of the MFC and the DLPFC in conflict resolution (Egner and Hirsch, 2005; Kerns, 2006; Kerns et al., 2004; MacDonald et al., 2000), and the observations that neural oscillations in the theta-band have been shown to underlie MFC/DLPFC-mediated conflict and error detection processes (Cavanagh et al., 2009; Cohen et al., 2008; Luu et al., 2004; Nigbur et al., 2012; Trujillo and Allen, 2007), our results suggest that conflict activates the MFC, irrespective of conflict awareness (transient "reactive" control) (D'Ostilio and Garraux, 2012). This local "obligatory" MFC activation can however carry over to the next trial (Fig. 3A), and therefore seems to have at least some potential for short term memory-like effects, but this is however related to the initiation of minimal conflict resolution mechanisms (van Gaal et al., 2010a). This is in accordance with models that pose that the MFC might actually exert cognitive control itself; broadly termed "the MFC regulatory theories" (Horga et al., 2011; Mansouri et al., 2009). These results suggest that strongly masked conflict information can be maintained in the MFC for at least around 1.2–1.5 s. However, the present results also show that, only when conflict is experienced fully consciously, the (left) DLPFC is recruited and conflict adaptation in behavior is strongly increased (more "selective" or "proactive" mode of processing). That this effect is left-lateralized is in line with previous fMRI (Kerns, 2006; Kim et al., 2013, 2014; Salami et al., 2014) and electrophysiological studies (Cavanagh et al., 2009; Cohen and van Gaal, 2013; Nigbur et al., 2012). However, other studies have also observed a role of the right DLPFC in conflict resolution, and whether the right or left DLPFC is found even varies while using the same paradigm (Egner and Hirsch, 2005; Greene et al., 2004; Kerns, 2006; Kerns et al., 2004). Overall, we hypothesize that the DLPFC might be crucial for actively holding the history of conflict information on-line and to implement optimal behavioral adaptations when the time between trials is prolonged, and that this process depends on conflict awareness.

We are aware that it is difficult to dissociate conflict adaptation effects from effects of repetition priming (Mayr et al., 2003) and feature integration (Hommel et al., 2004) especially in conflict task that involve a limited stimulus and response set (four possible stimulus pairs, two responses) (for reviews, see Duthoo et al., 2014; Egner, 2007; Schmidt, 2013), as used in the current study. However, although it has been argued and shown previously that these low-level effects can explain variance, previous studies have also observed that these conflict-related trial-by-trial effects cannot fully explain simple stimulus/response repetitions across trials (e.g., Oehrn et al., 2014; Ullsperger et al., 2005; van Gaal et al., 2010a). Further, in the present experiment, we carefully examined medial frontal and lateral frontal

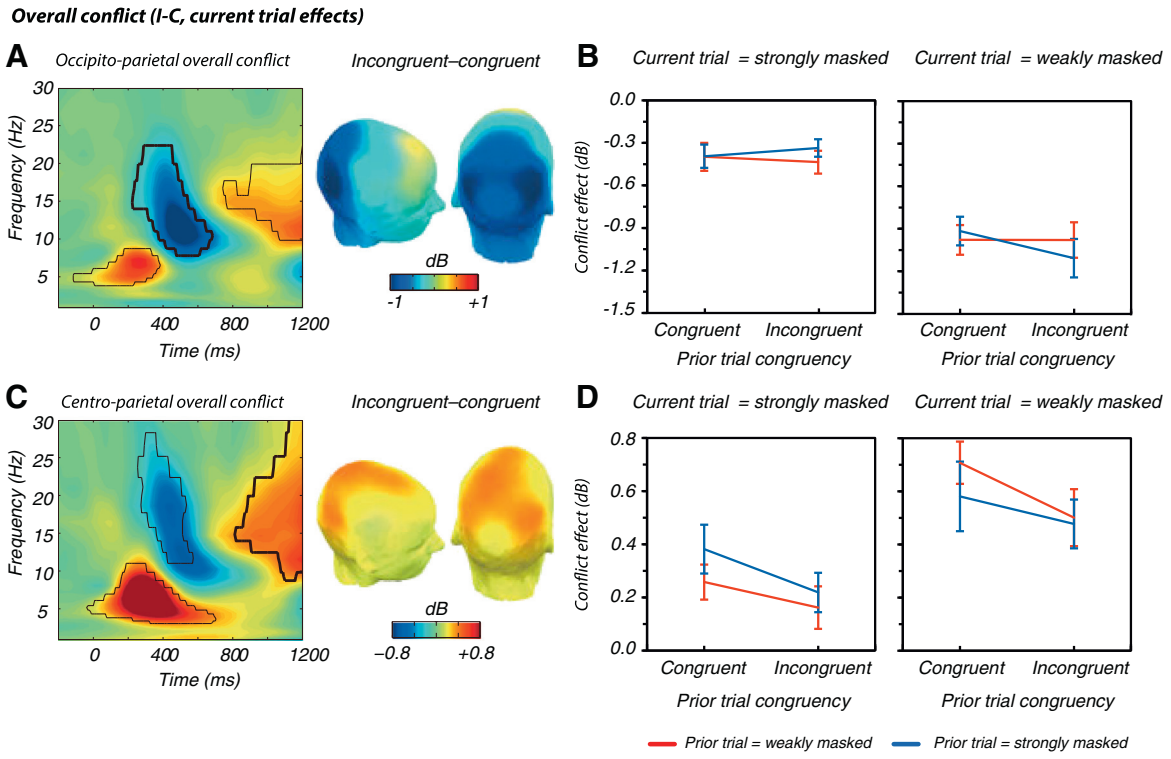


**Fig. 4.** Conflict effects for occipito-parietal alpha-band and centro-parietal beta-band power. (A) Time–frequency dynamics and topographical distributions for the overall conflict-related power decrease in alpha at occipito-parietal electrodes (230–680 ms). (B) Line plots for the alpha-band conflict effect at occipito-parietal electrodes, separated for masking strength on the prior and current trial and congruency on the prior trial. (C) Time–frequency dynamics and topographical distributions for the overall conflict-related power increase in the beta-band at centro-parietal electrodes (802–1200 ms). Black lines encircle regions of significance ($p < 0.001$, corrected for multiple comparisons using cluster-based statistics). The data (all T-F pixels) enclosed by thick black lines were used for topographical plots. (D) Line plots for the beta-band conflict effect at centro-parietal electrodes, separated for masking strength on the prior and current trial and congruency on the prior trial. A negative slope of the lines reflects a conflict adaptation effect.

theta-band neural dynamics that have been strongly linked to adaptive control mechanism (Botvinick et al., 2001; Mansouri et al., 2009). Therefore, we believe that it is likely that the reported results reflect conflict-control dynamics and not low-level repetition or feature integration effects, although future studies should address this issue in more detail.

In our more exploratory analyses we observed that central oscillatory beta-band power was increased by weakly masked conflict (and less so by strongly masked conflict), building up in the inter-trial-interval and peaking close upon stimulus presentation in the next trial (Fig. 4B/D). Although speculative, it might be that this beta-band oscillatory pattern reflects the actual memory trace of past conflict or a strategic control process building up in anticipation of the next trial (see also Horga and Maia, 2012; Horga et al., 2011). As suggested by Horga et al. (2011) and Horga and Maia (2012), inter-stimulus activation (in their case activation in the dorsal medial PFC and portions of the DLPFC) could reflect *reactive* memory processes that are passively activated by conflict, or *proactive* processes related to the anticipation of future conflict and the preparation of an optimal action strategy (see also Braver, 2012; Horga and Maia, 2012). Also, we observed an alpha-band decrease for conflict compared to no conflict on the current trial, which was stronger for weakly masked conflicting primes. Interestingly, these alpha and beta modulation were not influenced by conflict awareness in the prior trial; which was specific to theta-band modulations. The functional properties of alpha (i.e. "gating by inhibition", see reviews Jensen and Mazaheri, 2010) and beta (i.e. "signaling the status quo", see reviews Engel and Fries, 2010) during conflict resolution and adaptation are still unclear at present, and although these effects have been observed previously (Pastötter et al., 2013), and they need to be further explored in future studies. Also, future studies are necessary to further dissociate between a reactive vs. a proactive process in the inter-trial-interval, possibly by probing the temporal limitations of conflict adaptation under different inter-trial intervals. This is especially crucial considering the suggested passive and rapid decaying properties of subliminal information (Dehaene et al., 2006; Greenwald et al., 1996).

The present results might also explain why some behavioral studies have not observed conflict adaptation after subliminal conflict when the time between trials was relatively long (approximately >1.5 s), or when subjects were distracted or released their attentional focus in the inter-trial interval (e.g., Ansorge et al., 2011; Kunde, 2003). We have recently argued that the absence of conflict adaption in such situations might be related to the mnemonic aspects naturally involved in conflict adaptation (van Gaal et al., 2010a). In the present task, our masking procedure might not have rendered the primes fully unconscious, because the $d'$ prime measures showed that, with some effort and focus on the prime (which is not the case during main task performance), participants could discriminate the prime direction with above-chance performance. However, above-chance prime discrimination rules out the possibility that the absence of the DLPFC theta-band conflict adaptation effect on strongly masked conflict trials was due to an accidental lack of power ("too weak input"), especially because MFC-related theta-band effects were clearly observed after strongly masked conflict trials. Therefore, overall, MFC conflict-related activations seem to depend mainly on the strength and presence of conflict, but not necessarily the awareness thereof (D'Ostilio and Garraux, 2012; van Gaal et al., 2010b). On the other hand, DLPFC theta-band conflict adaptation modulations seem to have a more "all-or-none" profile (Dehaene et al., 2006) and might be uniquely present when conflict is experienced fully consciously.

## Acknowledgments

This work was supported by the National Natural Science Foundation of China (grant number 31470981), a VENI award from the Netherlands Organization for Scientific Research (NWO) to SvG and a Joint-PhD scholarship (No. 201306990046) of the China Scholarship Council (CSC) to JJ to study at the University of Amsterdam.

## Appendix A. Supplementary data

Supplementary data to this article can be found online at http://dx.doi.org/10.1016/j.neuroimage.2015.04.062.

## References

Ansorge, U., Fuchs, I., Khalid, S., Kunde, W., 2011. No conflict control in the absence of awareness. Psychological Research 75, 351–365.
Badgaiyan, R.D., 2000. Executive control, willed actions, and nonconscious processing. Hum. Brain Mapp. 9, 38–41.
Botvinick, M.M., Braver, T.S., Barch, D.M., Carter, C.S., Cohen, J.D., 2001. Conflict monitoring and cognitive control. Psychol. Rev. 108, 624–652.
Braver, T.S., 2012. The variable nature of cognitive control: a dual mechanisms framework. Trends Cogn. Sci. 16, 106–113.
Cavanagh, J.F., Frank, M.J., 2014. Frontal theta as a mechanism for cognitive control. Trends Cogn. Sci. 18, 414–421.
Cavanagh, J.F., Cohen, M.X., Allen, J.J.B., 2009. Prelude to and resolution of an error: EEG phase synchrony reveals cognitive control dynamics during action monitoring. J. Neurosci. 29, 98–105.
Cohen, M.X., van Gaal, S., 2013. Dynamic interactions between large-scale brain networks predict behavioral adaptation after perceptual errors. Cereb. Cortex 23, 1061–1072.
Cohen, M.X., van Gaal, S., 2014. Subthreshold muscle twitches dissociate oscillatory neural signatures of conflicts from errors. NeuroImage 86, 503–513.
Cohen, M.X., Ridderinkhof, K.R., Haupt, S., Elger, C.E., Fell, J., 2008. Medial frontal cortex and response conflict: evidence from human intracranial EEG and medial frontal cortex lesion. Brain Res. 1238, 127–142.
Cohen, M.X., van Gaal, S., Ridderinkhof, K.R., Lamme, V.A., 2009. Unconscious errors enhance prefrontal–occipital oscillatory synchrony. Front. Hum. Neurosci. 3, 54.
Compton, R.J., Arnstein, D., Freedman, G., Dainer-Best, J., Liss, A., 2011. Cognitive control in the intertrial interval: evidence from EEG alpha power. Psychophysiology 48, 583–590.
Compton, R.J., Huber, E., Levinson, A.R., Zheutlin, A., 2012. Is "conflict adaptation" driven by conflict? Behavioral and EEG evidence for the underappreciated role of congruent trials. Psychophysiology 49, 583–589.
D'Ostilio, K., Garraux, G., 2012. Dissociation between unconscious motor response facilitation and conflict in medial frontal areas. Eur. J. Neurosci. 35, 332–340.
Dehaene, S., Naccache, L., 2001. Towards a cognitive neuroscience of consciousness: basic evidence and a workspace framework. Cognition 79, 1–37.
Dehaene, S., Artiges, E., Naccache, L., Martelli, C., Viard, A., Schürhoff, F., Recasens, C., Martinot, M.L.P., Leboyer, M., Martinot, J.-L., 2003. Conscious and subliminal conflicts in normal subjects and patients with schizophrenia: the role of the anterior cingulate. Proc. Natl. Acad. Sci. 100, 13722–13727.
Dehaene, S., Changeux, J.-P., Naccache, L., Sackur, J., Sergent, C., 2006. Conscious, preconscious, and subliminal processing: a testable taxonomy. Trends Cogn. Sci. 10, 204–211.
Dehaene, S., Charles, L., King, J.-R., Marti, S., 2014. Toward a computational theory of conscious processing. Curr. Opin. Neurobiol. 25, 76–84.
Delorme, A., Makeig, S., 2004. EEGLAB: an open source toolbox for analysis of single-trial EEG dynamics including independent component analysis. J. Neurosci. Methods 134, 9–21.
Desender, K., Van Den Bussche, E., 2012. Is consciousness necessary for conflict adaptation? A state of the art. Front. Hum. Neurosci. 6, 3.
Desender, K., Van Lierde, E., Van den Bussche, E., 2013. Comparing conscious and unconscious conflict adaptation. PLoS One 8, e55976.
Duthoo, W., Abrahamse, E., Braem, S., Boehler, C.N., Notebaert, W., 2014. The heterogeneous world of congruency sequence effects: an update. Front. Psychol. 5.
Egner, T., 2007. Congruency sequence effects and cognitive control. Cogn. Affect. Behav. Neurosci. 7, 380–390.
Egner, T., Hirsch, J., 2005. Cognitive control mechanisms resolve conflict through cortical amplification of task-relevant information. Nat. Neurosci. 8, 1784–1790.
Eimer, M., Schlaghecken, F., 2003. Response facilitation and inhibition in subliminal priming. Biol. Psychol. 64, 7–26.
Engel, A.K., Fries, P., 2010. Beta-band oscillations—signalling the status quo? Curr. Opin. Neurobiol. 20, 156–165.
Gratton, G., Coles, M., Donchin, E., 1992. Optimizing the use of information: strategic control of activation of responses. J. Exp. Psychol. Gen. 121, 480–506.
Greene, J.D., Nystrom, L.E., Engell, A.D., Darley, J.M., Cohen, J.D., 2004. The neural bases of cognitive conflict and control in moral judgment. Neuron 44, 389–400.
Greenwald, A.G., Draine, S.C., Abrams, R.L., 1996. Three cognitive markers of unconscious semantic activation. Science 273, 1699–1702.
Hommel, B., 2007. Consciousness and control: not identical twins. J. Conscious. Stud. 14, 155–176.
Hommel, B., Proctor, R., Vu, K.-P., 2004. A feature-integration account of sequential effects in the Simon task. Psychological Research 68, 1–17.
Horga, G., Maia, T.V., 2012. Conscious and unconscious processes in cognitive control: a theoretical perspective and a novel empirical approach. Front. Hum. Neurosci. 6, 199.
Horga, G., Maia, T.V., Wang, P., Wang, Z., Marsh, R., Peterson, B.S., 2011. Adaptation to conflict via context-driven anticipatory signals in the dorsomedial prefrontal cortex. J. Neurosci. 31, 16208–16216.
Jack, A.I., Shallice, T., 2001. Introspective physicalism as an approach to the science of consciousness. Cognition 79, 161–196.
Jensen, O., Mazaheri, A., 2010. Shaping functional architecture by oscillatory alpha activity: gating by inhibition. Front. Hum. Neurosci. 4.
Jiang, J., van Gaal, S., Bailey, K., Chen, A., Zhang, Q., 2013. Electrophysiological correlates of block-wise strategic adaptations to consciously and unconsciously triggered conflict. Neuropsychologia 51, 2791–2798.
Kerns, J.G., 2006. Anterior cingulate and prefrontal cortex activity in an FMRI study of trial-to-trial adjustments on the Simon task. NeuroImage 33, 399–405.
Kerns, J.G., Cohen, J.D., MacDonald, A.W., Cho, R.Y., Stenger, V.A., Carter, C.S., 2004. Anterior cingulate conflict monitoring and adjustments in control. Science 303, 1023–1026.
Kim, C., Chung, C., Kim, J., 2013. Task-dependent response conflict monitoring and cognitive control in anterior cingulate and dorsolateral prefrontal cortices. Brain Res. 1537, 216–223.
Kim, C., Johnson, N.F., Gold, B.T., 2014. Conflict adaptation in prefrontal cortex: now you see it, now you don't. Cortex 50, 76–85.
Kunde, W., 2003. Sequential modulations of stimulus–response correspondence effects depend on awareness of response conflict. Psychon. Bull. Rev. 10, 198–205.
Luu, P., Tucker, D.M., Makeig, S., 2004. Frontal midline theta and the error-related negativity: neurophysiological mechanisms of action regulation. Clin. Neurophysiol. 115, 1821–1835.
MacDonald, A.W., Cohen, J.D., Stenger, V.A., Carter, C.S., 2000. Dissociating the role of the dorsolateral prefrontal and anterior cingulate cortex in cognitive control. Science 288, 1835–1838.
Mansfield, E.L., Karayanidis, F., Cohen, M.X., 2012. Switch-related and general preparation processes in task-switching: evidence from multivariate pattern classification of EEG data. J. Neurosci. 32, 18253–18258.
Mansouri, F.A., Buckley, M.J., Tanaka, K., 2007. Mnemonic function of the dorsolateral prefrontal cortex in conflict-induced behavioral adjustment. Science 318, 987–990.
Mansouri, F.A., Tanaka, K., Buckley, M.J., 2009. Conflict-induced behavioural adjustment: a clue to the executive functions of the prefrontal cortex. Nat. Rev. Neurosci. 10, 141–152.
Maris, E., Oostenveld, R., 2007. Nonparametric statistical testing of EEG- and MEG-data. J. Neurosci. Methods 164, 177–190.
Mayr, U., Awh, E., Laurey, P., 2003. Conflict adaptation effects in the absence of executive control. Nat. Neurosci. 6, 450–452.
Mognon, A., Jovicich, J., Bruzzone, L., Buiatti, M., 2011. ADJUST: an automatic EEG artifact detector based on the joint use of spatial and temporal features. Psychophysiology 48, 229–240.
Nigbur, R., Ivanova, G., Stürmer, B., 2011. Theta power as a marker for cognitive interference. Clin. Neurophysiol. 122, 2185–2194.
Nigbur, R., Cohen, M.X., Ridderinkhof, K.R., Stürmer, B., 2012. Theta dynamics reveal domain-specific control over stimulus and response conflict. J. Cogn. Neurosci. 24, 1264–1274.
Norman, D., Shallice, T., 1986. Attention to action: willed and automatic control of behavior. In: Davidson, R.J., Schwartz, G.E., Shapiro, D. (Eds.), Consciousness and Self-regulation. Plenum, New York, pp. 1–18.
Oehrn, C.R., Hanslmayr, S., Fell, J., Deuker, L., Kremers, N.A., Do Lam, A.T., Elger, C.E., Axmacher, N., 2014. Neural communication patterns underlying conflict detection, resolution, and adaptation. J. Neurosci. 34, 10438–10452.
Pastötter, B., Dreisbach, G., Bäuml, K.-H.T., 2013. Dynamic adjustments of cognitive control: oscillatory correlates of the conflict adaptation effect. J. Cogn. Neurosci. 25, 2167–2178.
Posner, M., DiGirolamo, G., 1998. Executive attention: conflict, target detection, and cognitive control. In: Parasuraman, R. (Ed.), The Attentive Brain. MIT Press, Cambridge, pp. 401–423.
Roelofs, A., van Turennout, M., Coles, M.G.H., 2006. Anterior cingulate cortex activity can be independent of response conflict in Stroop-like tasks. Proc. Natl. Acad. Sci. U. S. A. 103, 13884–13889.
Salami, A., Rieckmann, A., Fischer, H., Bäckman, L., 2014. A multivariate analysis of age-related differences in functional networks supporting conflict resolution. NeuroImage 86, 150–163.
Schmidt, J., 2013. Questioning conflict adaptation: proportion congruent and Gratton effects reconsidered. Psychon. Bull. Rev. 20, 615–630.
Tadel, F., Baillet, S., Mosher, J.C., Pantazis, D., Leahy, R.M., 2011. Brainstorm: a user-friendly application for MEG/EEG analysis. Comput. Intell. Neurosci. 2011, 13.
Tang, D., Hu, L., Chen, A., 2013. The neural oscillations of conflict adaptation in the human frontal region. Biol. Psychol. 93, 364–372.
Trujillo, L.T., Allen, J.J.B., 2007. Theta EEG dynamics of the error-related negativity. Clin. Neurophysiol. 118, 645–668.
Ullsperger, M., Bylsma, L.M., Botvinick, M.M., 2005. The conflict adaptation effect: it's not just priming. Cogn. Affect. Behav. Neurosci. 5, 467–472.
van Driel, J., Ridderinkhof, K.R., Cohen, M.X., 2012. Not all errors are alike: theta and alpha EEG dynamics relate to differences in error-processing dynamics. J. Neurosci. 32, 16795–16806.
van Gaal, S., Lamme, V.A.F., 2012. Unconscious high-level information processing: implication for neurobiological theories of consciousness. Neuroscientist 18, 287–301.

van Gaal, S., Lamme, V.A.F., Ridderinkhof, K.R., 2010a. Unconsciously triggered conflict adaptation. PLoS One 5, e11508.
van Gaal, S., Ridderinkhof, K.R., Scholte, H.S., Lamme, V.A.F., 2010b. Unconscious activation of the prefrontal no-go network. J. Neurosci. 30, 4143–4150.
van Gaal, S., Scholte, H.S., Lamme, V.A.F., Fahrenfort, J.J., Ridderinkhof, K.R., 2011. Pre-SMA gray-matter density predicts individual differences in action selection in the face of conscious and unconscious response conflict. J. Cogn. Neurosci. 23, 382–390.
Wickens, T.D., 2002. Elementary Signal Detection Theory. Oxford University Press, Oxford.